2016 IEEE 55th Conference on Decision and Control (CDC)
ARIA Resort & Casino
December 12-14, 2016, Las Vegas, USA

A Dynamical Systems Approach to Obstacle Navigation for a Series-Elastic Hexapod Robot

Matt Travers, Alex Ansari, and Howie Choset

***Abstract*— This paper emphasizes reliability in designing controllers to enable a blind, modular series-elastic hexapod robot to autonomously navigate (climb over) obstacles such as steps and curbs. Specifically, we suggest that it is not only important to limit the complexity of controllers, but also to limit the number of operating controllers to reduce potential failure points. As such, this paper presents a two-tiered control scheme with a high-level behavioral and a mid-level, modified admittance controller. The behavioral controller, based on a dynamical systems approach, is easy to implement – it is model-less, and may be realized using only analog circuitry. At its core, two oscillators coordinate the phasing of the robot's legs in open loop for nominal locomotion and climbing behaviors. A simple bistable dynamical system accepts torque feedback to decide the active mode and smoothly transition between behaviors – an alternating tripod gait for nominal walking and a quadrupedal gait in climbing mode. Finally, the mid-level, modified admittance controller naturally generates discrete motions as a byproduct of regulating compliant interactions. The proposed controller avoids unnecessary complexities that would be required in switching between discrete motion controllers or primitives in a state machine. It allows the robot to adapt to different obstacle heights while minimizing open parameters.**

I. Introduction

To support real-time operations in unstructured terrains, such as those necessary in urban search and rescue, a control scheme should not be overly complex. That is, it is important to limit the number of points of failure and parameters for calibration and performance tuning, which may be required on-site. To these ends, this paper proposes an approach that combines open-loop gaits with closed-loop compliance to allow a blind hexapod robot to autonomously navigate (climb over) obstacles using only angular encoders and proprioceptive force feedback.

The proposed scheme is implemented on a hexapod robot composed of series elastic actuator (SEA) modules [8] (see Fig. 1). While not particularly fast, the robot's compliant legs provide the potential to navigate complex environments where wheeled and stiff-jointed platforms cannot robustly enter. For search and rescue, the SEA hexapod's topology is also beneficial in that 1) the leg SEA modules can withstand forceful impacts; 2) the modules are interchangeable and easily replaced; and 3) the robot has natural redundancy, capable of locomotion with only 4 legs. We also leverage sensor redundancy for added robustness, using proprioceptive feedback from joint-torque sensors located in each module.

M. Travers, A. Ansari, and H. Choset are with the Robotics Institute at Carnegie Mellon University, Pittsburgh, PA 15213, USA. {mtravers@andrew, aansari1@andrew, choset@cs}.cmu.edu

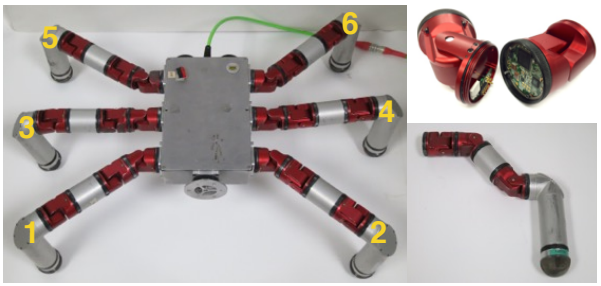

Fig. 1: Series-elastic actuated (SEA) hexapod robot. The legs are numbered beginning from the right-front of the robot's body. Each leg has three single degree-of-freedom (DOF) rotational joints (SEA actuated) and two passive elements, one of which has a rubberized "foot." The proximal joint provides a yaw DOF, and the medial and distal joints each provide a pitch DOF relative to the robot's body.

To control the SEA hexapod, this paper proposes both a high-level behavioral and a mid-level leg compliance controller. First, we take a dynamical systems approach to high-level behavior specification that minimizes computational resources. The proposed controller uses phase oscillators to coordinate open-loop desired behaviors, corresponding to a hexapod alternating-tripod gait for nominal locomotion and a quadrupedal gait for climbing. Rather than discretely switching between these behaviors when an obstacle is encountered, we design a neuronal model that requires only joint-torque information to transition behaviors. Using the front legs as antenna, sensed torques are fed back into a bistable dynamical system that governs the state of a single parameter that transitions from nominal locomotion to climbing upon obstacle detection. Effectively, we provide a single parameter compliant dynamical switch that smoothly transitions between limit cycles that coordinate different behaviors. To our knowledge, this strategy for low-dimensional, smooth behavioral switching is unique to this work.

As described in Section II, the proposed behavioral controller is similar in spirit and provides many of the benefits of central pattern generators (CPGs) [7], e.g., smooth transitions and stable limit cycle behavior, but is easier to implement. Each limit cycle behavior evolves according to an individual oscillator rather than CPG networks of oscillators. Hence, there is no need to identify matrices of stabilizing coupling parameters required to converge to desired joint phase offsets in CPGs. Similarly, joint motions during behavioral transitions are intuitive and easy to design, since the dynamics of these motions are not tied to the stability properties of an entire network.

978-1-5090-1836-9/16/$31.00 ©2016 IEEE

To navigate ledges, curbs, and steps that are too high for the robot to step over, the SEA hexapod performs several discrete actions for alignment and leg clearance. Rather than divide the climbing behavior into smaller, discrete motion phases, i.e. as in a state machine approach, our mid-level, modified admittance controller automatically generates and phases these discrete motions as the natural result of regulating limb compliance. A single additional reflex response, which modifies the admittance properties of the controller during execution, is sufficient for autonomous obstacle navigation.

Augmenting the open-loop quadruped gait in climbing, the mid-level controller ensures the SEA hexapod's motions are adaptive to the environment and obstacle geometry. Experiments show the resulting behaviors are more robust and much more effect than simple "canned" motions. Also, by avoiding the need to design, tune, and switch between multiple controllers in climbing, the proposed low-level control scheme improves reliability and eases implementation.

Following this Introduction, Section II provides a background on related works. Section III describes the mid-level compliant behavioral controller. Section IV discusses the low-level admittance controllers. Experimental results are in Section V with conclusions in Section VI.

II. Related Works

The control approach described in this paper is predicated on the idea that complex behaviors can be composed of simple primitives. For instance, we generate both walking and obstacle climbing behaviors by layering relatively straightforward closed-loop policies on top of simple open-loop gait cycles. While one may question whether open-loop gaits provide sufficiently robust base controllers for climbing, we highlight prior work that motivates our proposed approach.

In particular, [11] cites biological evidence that suggests that animals may utilize open-loop strategies during locomotion. The authors conduct a series of locomotion experiments for Cheeta-cub, a compliant quadruped robot, in which they set a record for quadruped trotting speed using only a simple open-loop gait. The authors highlight the self-stabilizing properties of their robot's compliant design and emphasize their belief that locomotion (on flat terrain) should be performed "almost blindly", without sensory feedback or explicit models. They show the same controller successfully navigates steps ranging from 7.5%-20% of their robot's standing hip height (20% success rate at the 20% step height). Here, we build on these concepts, similarly leveraging our robot's compliant properties and adding feedback controllers for more aggressive step climbing tasks with step heights that reach the underside of our robot.

In [11], the open-loop trajectory for Cheeta-cub's legs is synthesized by a central pattern generator (CPG). CPGs are neural circuits in animals that generate rhythmic signals without the aid of the peripheral nervous system. They coordinate rhythmic activities in animals, e.g., walking, and have become a popular tool in robotic motion control. In robotics, CPGs are typically implemented as networks of coupled oscillators. When properly designed, these networks yield rhythmic signals with desired phase offsets to coordinate robotic gaits and have desirable properties such as phase locking, mechanical entrainment, and stable limit cycles. However, design of CPGs networks, specification of coupling terms, and incorporation of feedback prove challenging as the field lacks formal tools and well-established methods [7].[1]

While open-loop CPG implementations avoid difficulties in integrating feedback, they no longer benefit from mechanical entrainment and merely provide phase coordinated joint signals. As opposed to using simple sine generators, CPGs still exhibit stable limit cycles and so may be utilized, as in [11], to provide smooth motion transitions from initial conditions to the desired limit cycle. The gait control scheme implemented here is similar to such an open-loop CPG scheme in that it coordinates legs based on several (two) nonlinear oscillators. However, as each oscillator coordinates a separate behavioral phase, we avoid the complications involved in specifying CPG coupling parameters. Our approach is easy to implement and still provides smooth motion transitions between behaviors.

In addition to [11], several authors have utilized CPGs in both open and closed-loop implementations for locomotion control. Most related to our work, [3] presents a bio-inspired controller that switches between different types of gaits on a hexapod. They use a CPG to coordinate the legs and modulate the CPG with a drive signal that is mapped to different sets of CPG parameters for starting, stopping, and transitioning between different gaits. A parallel controller provides feedback to compensate for lateral inclination using a dynamical system to regulate leg height. The system extends legs in the direction toward which the robot is tiled and folds others to reduce lateral tilt. Results are demonstrated on a simulated Chiara hexapod.

A more complex approach in [5] combines CPGs, backbone joint control, leg reflexes, and neural learning to generate adaptive walking and climbing behaviors similar to those considered here. However, climbing is not blind. Experiments use ultrasonic, foot contact, and infrared sensors, to enable a hexapod robot to adapt while climbing steps and curbs up to 75% of leg length (in the peak, high-friction indoor case; lower outdoors). As the mentioned in [5], there are wheel-legged robots, e.g., Rhex [10], that can overcome obstacles that are higher with respect to leg length, but these robots tend to have fewer degrees of freedom and thus motion capabilities that are not comparable.

Furthermore, [9] introduces a new CPG model for hexapod robots that allows a superposition of discrete and rhythmic primitives. The authors conduct a simulation study that shows in certain cases it is possible to superimpose discrete and rhythmic primitives in a manner that leaves amplitude and frequency constant. They suggest this may facilitate the design of more complex motions to allow hexapod robots to accommodate more complicated terrains since joint offset can be affected without changing the amplitude and

[1]For a review of CPGs in the context of locomotion control see [7].

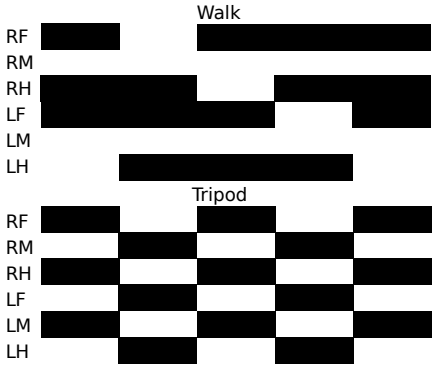

Fig. 2: The step pattern for walking and tripod gaits. The black rectangles indicate when each foot is on the ground (L/R for left / right and F/H for front / hind leg).

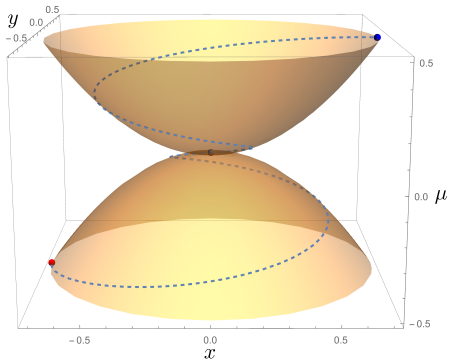

Fig. 3: Smooth transitioning between the limit cycles of two nonlinear oscillators by varying μ. The blue sample trajectory results when μ is linearly reduced from 0.5 to -0.5.

frequency of rhythmic motion in such cases.

In the case of quadrupeds, both [4] and [2] use CPG-based controllers to facilitate walking over irregular terrain. As with [11], the authors converge on a leg flexion / extension reflex controller to account for unexpected bumps and drops, and both modulate joint stiffness using either a virtual spring-damper system [4] or virtual model control [2]. The CPG controller in [4] is provided with sensed rolling motion as feedback to mutually entrain this motion with that of the virtual leg spring-dampers. Experimental results in [4] include a robot (Tekken) that can walk over steps up to 20% of leg length and slopes of up to 10°. The controllers in [2] are validated in simulation. Again, simulations show successful walking for steps up to 20% of leg length and slopes of 20% (up to 36.5% with a lower success rate).

Most of these prior works focus on locomotion considering modest terrain variation, with some hexapod results (often in simulation) that rely on complex controllers for climbing over larger obstacles. This paper focuses on using few, relatively straightforward, and low-dimensional control policies to achieve aggressive step climbing behaviors with step heights approximately equal to the robot's standing height (88% of leg length). We demonstrate our results experimentally on a modular SEA robot. We leverage the compliance in the robot's modular actuators and show even noisy torque feedback provided by SEA actuators can be used to regulate effective environmental interactions.[2]

III. Behavioral Control

Both the nominal walking as well as climbing behaviors for the SEA hexapod are based on open-loop gaits in which phase oscillators coordinate the desired joint relationships. For nominal walking, an alternating tripod gait is used (see [6], [9]). As shown in Fig. 2, the gait consists of two sets of three legs – a pair of ipsilateral fore and hind legs combined with the contralateral middle leg. The legs in each of these tripods move synchronously, while the two tripods remain half a gait cycle out of phase. As such, one leg group is in swing (in the air) while the remaining three legs are on the ground for support.

The climbing behavior is built around a quadrupedal walking gait (see Fig. 2). This gait requires only the robot's fore and hind legs and leaves the middle legs free for use in a reactive control scheme that aligns the robot and provides support to improve climbing reliability. The walking gait leaves three legs on the ground while the fourth is in swing and enforces a quarter cycle phase lag between legs – left hind, left fore, right hind, and right fore [6].

Though both the hexapod and quadrupedal gaits can be implemented in closed-loop using foot switches to detect contact, based on desired search and rescue applications, we chose to minimize reliance on external sensors not included on every module. This design uses redundancy to reduce sensitivity to sensor failures and ensures sensors are modular and easily replaced. Thus, in both cases, the SEA hexapod's gaits are implemented in open-loop. In contrast to the typical approach adopted in the CPG community, we define static phase lags for the legs around a single centralized phase oscillator in each of the two operational modes.

The phase oscillator equations for each the nominal as well as climbing behaviors are based on Hopf oscillator equations, i.e., in polar coordinates,

$$\dot{r}_w = (\mu - r_w^2) r_w \tag{1}$$
$$\dot{\theta}_w = \omega_w$$
$$\dot{r}_c = (-\mu - r_c^2) r_c \tag{2}$$
$$\dot{\theta}_c = \omega_c,$$

where the radii, r_w and r_c, and phase variables, θ_w and θ_c, correspond to the walking and climbing behaviors respectively. The bifurcation parameter μ sets the stability properties for each behavior; notice the opposite sign of μ in (1) and (2). We use the phase space (r, θ, μ) to provide an associated radius, r, and phase, θ, for each behavior as a function of μ. These parameters are used to set the desired feed-forward joint angles of the robot during real-time operation. For example, considering the SEA hexapod shown in Fig. 1, with joint angles $\phi \in \mathbb{R}^{18}$, the gait functions for walking and climbing f define $\phi_g = r_g(\mu) \cdot f_g(\theta_g) + \phi_0$

[2]We use joint torques as feedback for mid-level leg admittance and high-level compliant behavioral switching controllers.

for $g \in \{w, c\}$ and where ϕ_0 is the desired nominal stance at the point $r_c = r_w = \mu = 0$.

In terms of stability properties for walking and climbing, (1) and (2) are designed so that a dual bifurcation occurs at the origin. Switching the sign of μ causes the emergence of limit cycle behavior in one system, and its collapse in the other. That is, when μ is a positive value, (1) has an unstable node and stable limit cycles at $r = \{0, \pm\sqrt{\mu}\}$, while (2) has a single stable node at $r = 0$.[3] The opposite is true when the sign of μ is negative. We use this alternating stability property as the basis for switching behaviors from climbing to walking, and back again, in our behavioral controller.

The switched stability properties of our behavioral controller are presented graphically in Fig. 3. Assume the upper convex lobe in Fig. 3 corresponds to the stable limit cycle (as a function of μ) of the Hopf oscillator governing the tripod walking gait (controlled by (r_w, θ_w)). The blue sphere indicates a point on the stable limit cycle when $\mu_w = 0.5$. In Cartesian coordinates, with $x_i = r_i \cos(\theta_i)$ and $y_i = r_i \sin(\theta_i), i \in \{w, c\}$, the oscillator depicted evolves along a circle of radius $\sqrt{0.5}$ as long as the μ remains fixed. Assuming that some transition forces the value of μ to approach zero, the dashed blue line on the surface of the upper lobe in Fig. 3 traces a potential path through the behavioral phase space, eventually reaching the origin.

Continuing to decrease the value of μ, i.e., $\mu < 0$, the system will transition to the stable cycle of (2), which coordinates the quadrupedal gait that we use as the basis for climbing.[4] The concave lobe in Fig. 3 depicts the phase space of stable quadrupedal limit cycles. Assuming that μ is decreased until it reaches $\mu = -0.5$, the dashed-blue line on the concave lobe in Fig. 3 traces one potential path through the quadrupedal gait phase space. This gait will eventually settle into a stable limit cycle with a radius of $\sqrt{0.5}$.[5] The red sphere in Fig. 3 indicates a point on this limit cycle.

A. A Compliant Dynamical System to Transition Behaviors

To reliably switch behaviors from walking to climbing and remain robust to sensor noise and failures, we use a neural-inspired model to queue the transition from walking to climbing. That is, rather than switching based on a single threshold sensor value, the behavioral switching is based on a model that integrates torques sensed at the SEA joints. If the integrated sensory signal reaches a threshold, a discrete "firing" event triggers the associated behavioral switch.

For example, Fig. 4 shows experimentally measured torque signals from the proximal joints on the two front legs of the system, τ_p^1 and τ_p^2 respectively (see Fig. 1). The robot is initially walking in an unconstrained part of the environment,

[3]Technically, $r = 0$ corresponds to stable zero amplitude limit cycle unless $\omega = 0$. However, because the joint angles follow r, the robot remains fixed when $r = 0$ and ω has no effect.

[4]Note that $r_w \to 0$ as $\mu \to 0$. Allowing the radius to become negative, the stable limit cycles for (2) reflect about the Cartesian x, y and μ axes relative to those of (1). The sample path in Fig 3 demonstrates the design yields smooth transitions through the origin.

[5]The parameters of (1) and (2) may be chosen differently, in which case the two lobes would not be symmetric.

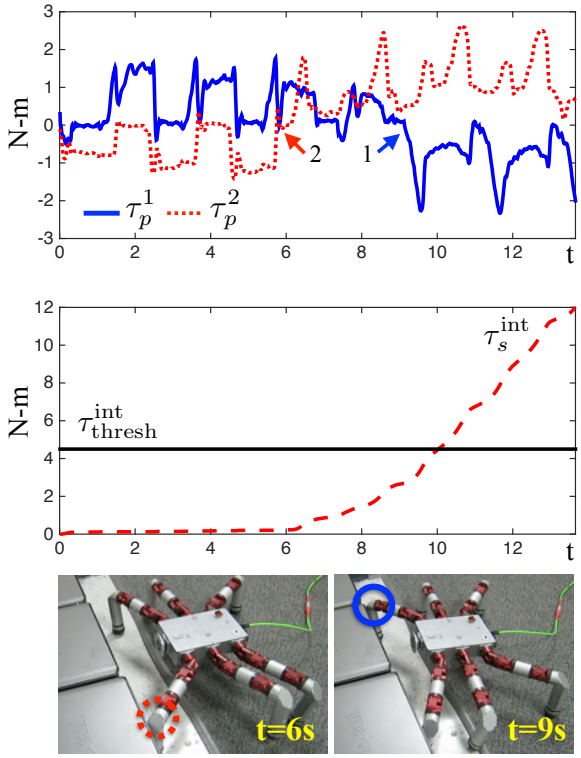

Fig. 4: Transition from walking to climbing using only proprioceptive sensing in the SEA hexapod's front legs.

but contacts an obstacle with leg 2 at $t \approx 6$s. The obstacle exerts a force on the leg that counteracts the propulsive force of the gait, and subsequently forces τ_p^2 to reverse signs. For a period of time after $t \approx 6$s, leg 1 continues stepping in free space due to the fact that the robot is not initially aligned with the obstacle. By continuing the walking gait, the system naturally pivots around the leg 2 contact and eventually aligns itself so that leg 1 also contacts the obstacle ($t \approx 9$).

The reversal of signs in the two torque signals, τ_p^1 and τ_p^2, caused by the reaction forces imposed by the obstacle, is used as the basis for triggering the dynamic switch in behaviors between walking and climbing. Specifically, a combined signal of the two torque signals is defined as, $\tau_s = \max(0, \tau_p^1) - \min(0, \tau_p^2)$, which discards values of τ_p^1 and τ_p^2 during unconstrained walking. To filter as well as build a time history of the measured torques, τ_s is integrated with respect to time using an Euler integration scheme, producing τ_s^{int}. A threshold value is defined and used to signal the point at which the behavior of the system switches from walking to climbing. The value of the threshold is user defined, and is set high enough to allow the system to orientate itself to the obstacle before attempting to climb.

When a behavioral transition is enabled, linear dynamics are used to shape the response of the bifurcation parameter, μ, to ensure smooth transitions. In particular, we define second-order linear dynamics

$$M\ddot{\mu} + B\dot{\mu} + K(\mu - \mu_r) = 0, \tag{3}$$

where the effective mass, M, damping, B, and spring constant, K, stabilize the system to a desired reference, μ_r.

When the neural trigger is fired, e.g., when $\tau_s^{\text{int}} = \tau_{\text{thresh}}^{\text{int}}$, the reference parameter, $\mu_r \in \{\mu_{r,w} > 0, \mu_{r,c} < 0\}$ discretely switches values. The stabilizing dynamics in (3) then cause the value of μ to converge to μ_r with a step response governed by the parameters M, B, and K.

An advantage of the behavioral controller described in this section is that it is easy to implement. That is, it requires only proprioceptive sensing and minimal computation. In cases of software implementation, the stable limit cycles can be computed analytically. Also, since Hopf oscillators and μ dynamics can be realized in hardware [1], it is possible to implement the proposed behavioral control using entirely analogue circuitry.

IV. Climbing Behavior Adaptation

The behavioral switch discussed in Section III switches the SEA hexapod into a climbing behavior, which is coordinated around a quadrupedal walking gait. Without additional regulation, the open-loop quadrupedal gait is unable to carry the system over steep obstacle heights reaching higher than the maximum swing height of the its feet (≈ 10 cm). To allow the robot to adapt to obstacles of unknown sizes during climbing, we augment the open-loop gait with compliant control. Specifically, the SEA hexapod uses a modified admittance controller that runs in parallel with the quadrupedal gait to adapt leg heights to terrain variations. A single compliant reflex response switches the sign of the admittance controller to swing the robot's back legs onto the obstacle in the terminal stages of the climbing mode.

For dimensionality reduction, we constrain the vertically rotating medial and distal joints of each leg such that $\theta_m^i = -\theta_d^i, i \in \{1, \ldots, 6\}$. The i superscript indicates the leg number (see Fig. 1) and the subscripts indicate medial and distal joints. This constraint ensures the desired orientation of each leg remains normal to the horizontal body plane and enables the height of each leg to be controlled using a single parameter. Furthermore, we assume the height of contralateral legs to be coupled. These assumptions allow the complaint controller to be reduced to controlling four signals, $q = (q_1, q_2, q_3, q_4)$ representing the height of the front, middle, and hind leg pairs, as well as an additional term that affects the height of the middle legs, respectively.

The dynamics of the admittance controller governing the evolution of q have the form,

$$M_q \ddot{q} + B_q \dot{q} + K_q(q - q_r) = F_q, \tag{4}$$

where M_q, B_q, and K_q are an effective mass, damping, and spring constant, and F_q is an effective force acting on each of the signals. The q_r term corresponds to the nominal position of q, i.e., the reference value of q in the absence of external forcing. The reference values are set to $q_r = 0$. The effective force term is calculated by mapping measured joint torques distributed throughout the different leg pairs into their respective q_i's.

To successfully climb, the dynamics in (4) need to coordinate several different discrete motion sequences at different phases of the behavior. The components of the forcing term

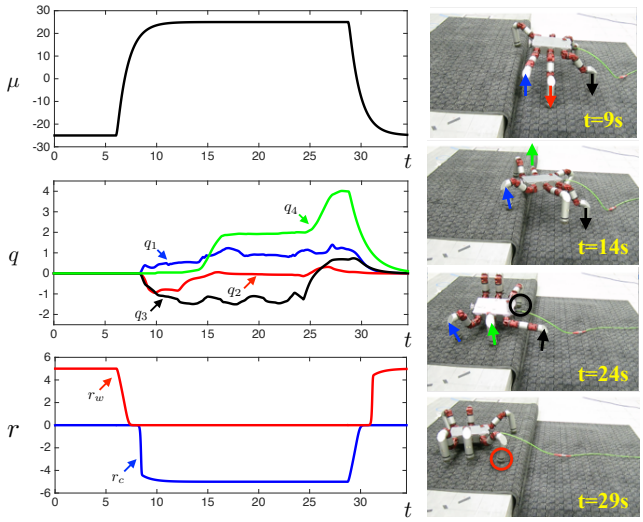

Fig. 5: Sequence of the SEA hexapod encountering an obstacle while walking ($t \approx$ 6s), transitioning to climbing, compliantly controlling its leg heights (q_1, q_2, q_3, q_4), to navigate over the obstacle, and transitioning back into walking ($t \approx 29$s).

F_q are defined so that each of the discrete motions happen naturally. For example, in the first phase of climbing, the body of the system needs to raise high enough to enable the front legs to swing on top of the obstacle (see picture in Fig. 5 at $t = 9$s). This motion results from defining F_q^2 and F_q^3 to provide positive feedback, causing them to counteract ground reaction forces, i.e., causes leg-height extension, during stance. Specifically $F_q^2 = -J^v \cdot (\tau^3 + \tau^4)$ and $F_q^3 = -J^v \cdot (\tau^5 + \tau^6)$, where $J^v = [0, 1, -1]$ and $\tau^3, \tau_4, \tau^5, \tau_6 \in \mathbb{R}^3$ are vectors containing the measured joint torques in the three joints of legs $3, 4, 5$ and 6 respectively (see Fig. 1). Additionally, defining F_q^1 to provide negative feedback, i.e., $F_q^1 = J^v \cdot (\tau^1 + \tau^2)$, where τ^1 and τ^2 are the joint torques measured in legs 1 and 2 respectively, causes the front legs to comply to the ground reaction forces, which acts to adjust the robot's body pitch such that it remains parallel to the ground during this portion of the behavior (see the plot of $q_{1,2,3}$ and the picture of the robot at $t = 9$s in Fig. 5).

The second phase of the climbing behavior aims to get the robot's middle legs onto the obstacle. With the robot's front legs on top of the obstacle, the system is primarily braced by the front and hind legs in this phase. As the magnitude of F_q^3 decreases, the positive feedback policy eventually lifts the middle legs off the ground. As the middle legs lift, the system walks forward until one of the middle legs contacts the obstacle, as shown in the picture in Fig. 5 at $t = 14$s. The contact helps to stabilize and align the robot to the obstacle. Also, as the reaction forces exerted by the obstacle on the middle legs grows, the forcing terms F_q^4, defined by $F_q^4 = J^h \cdot (\tau_5 - \tau_6))$ with $J^h = [1, 0, 0]$, causes the admittance control policy for q_4 to raise the middle legs until they clear the obstacle (see plot of q_4 in Fig. 5). Note that the height of the middle legs is the sum of $q_2 + q_4$, where the height of the front and hind legs correspond to q_1 and q_3, respectively.

In the third and final phase of the climbing gait, a reflex response switches the sign of F_q^3 (which governs the height of the back feet) when the joint torque sensors in the hind legs indicate touchdown of either hind foot on the top of the obstacle. The reversed compliance property causes the robot to adjust its stance until its body becomes parallel with the plane on top of the obstacle. This reflexive switch provides sufficient clearance for the remaining hind foot to robustly step up and onto the obstacle, as shown in Fig. 5 ($t = 24$s).

Sensory feedback from touchdown of the robot's remaining hind foot updates the behavioral controller's reference value, μ_r. The updated reference initiates the transition back to nominal hexapod walking (see $t = 29$s in Fig. 5).

V. Experimental Results

Experimental trials focused primarily on indoor environments with a variety of obstacles including carpeted steps of varying heights and toppled desktop computers. A total of ten experiments were conducted per step height with heights of 17, 20, and 22cm, which correspond to 68%, 80%, and 88% of the robot's effective leg height. In each case, we set the robot in a position that was approximately one half meter away from the obstacle and orientated so that the robot would walk toward the obstacle. The robot successfully traversed the obstacle in all cases using the same parameter values. Sample results are included in Fig. 5 and at https://youtu.be/zJRqJIziJmE.

In addition to the relatively high-friction indoor trials, we conducted preliminary tests of the robot in several different outdoor environments (similar to those from [5]). These trials show that the robot can successfully navigate over curbs up to 20cm (80% of effective leg height). However, these results were unreliable and highly dependent on terrain factors. Dust, dirt, and sand made it difficult for the robot to walk during its approach, as the stance feet would slide uncontrollably during horizontal abduction. Similar problems occurred while climbing, as the robot's feet would slide off the top of curbs. To address these issues, we intend to consider new, more robust foot designs for outdoor environments, as discussed in Section VI. Examples of successful outdoor trials are included in the video https://youtu.be/zJRqJIziJmE.

VI. Conclusions

This paper suggests that to provide reliable performance and minimize potential on-site issues such as calibration and tuning, controllers should be few and simple, i.e., avoiding complex models and open parameters. To these ends, we design a control scheme that enables a hexapod robot to climb over a variety of steps and ledges. The approach combines simple limit cycle behaviors (gaits) with a compliance policy that automatically generates a sequence of required discrete actions. While the compliant policy requires intuition to design, experiments show the approach works reliably, allowing the robot to react flexibly and adaptively to the environment. Using the proposed controllers, the hexapod successfully climbs over different obstacles, e.g. toppled computers cases, steps, and curbs, without precise positioning or initial conditions. These results do not require precise tuning and can be achieved with the same parameters.

We note that the single parameter compliant dynamical switch, applied here for low-dimensional control of behavioral transitions, is general and not limited to two limit cycles. In future work, we will explore using a similar framework to transition between arbitrary numbers of limit-cycle-regulated modes using feedback to modify the evolution of the single switching parameter, μ. To improve performance in low-friction environments, future work will also address hardware design issues pertaining to the SEA hexapod's feet. Specifically, we intend to experiment with compliant foot designs with increased surface area. The current feet (rubber hemispheres) provide relatively small contact surfaces that do not deform sufficiently and slip over loose debris.

ACKNOWLEDGMENT

The authors would like to thank the Robotics Collaborative Technology Alliance (RCTA) program supported through the United States Army Research Lab (ARL) for its support of this work.

References

[1] A. Ahmadi, E. Mangieri, K. Maharatna, S. Dasmahapatra, and M. Zwolinski. On the VLSI implementation of adaptive-frequency Hopf oscillator. *IEEE Transactions on Circuits and Systems I: Regular Papers*, 58(5):1076–1088, May 2011.

[2] Mostafa Ajallooeian, Sébastien Gay, Alexandre Tuleu, Alexander Spröwitz, and Auke Ijspeert. Modular control of limit cycle locomotion over unperceived rough terrain. In *Proc. IEEE Conf. Intelligent Robots and Systems*, pages 3390–3397. IEEE, 2013.

[3] Ricardo Campos, Vitor Matos, and Cristina Santos. Hexapod locomotion: A nonlinear dynamical systems approach. In *Proc. IEEE Conf. Ind. Electron. Soc.*, pages 1546–1551. IEEE, 2010.

[4] Yasuhiro Fukuoka, Hiroshi Kimura, and Avis Cohen. Adaptive dynamic walking of a quadruped robot on irregular terrain based on biological concepts. *The International Journal of Robotics Research*, 22(3-4):187–202, 2003.

[5] Dennis Goldschmidt, Florentin Wörgötter, and Poramate Manoonpong. Biologically-inspired adaptive obstacle negotiation behavior of hexapod robots. *Frontiers in neurorobotics*, 8, 2014.

[6] Martin Golubitsky, Ian Stewart, Pietro-Luciano Buono, and J.J. Collins. A modular network for legged locomotion. *Physica D: Nonlinear Phenomena*, 115(1):56–72, 1998.

[7] Auke Jan Ijspeert. Central pattern generators for locomotion control in animals and robots: a review. *Neural Networks*, 21(4):642–653, 2008.

[8] Simon Kalouche, David Rollinson, and Howie Choset. Modularity for maximum mobility and manipulation: Control of a reconfigurable legged robot with series-elastic actuators. In *IEEE Safety, Security, and Rescue Robotics*, October 2015.

[9] Carla Pinto, Diana Rocha, and Cristina Santos. Hexapod robots: new CPG model for generation of trajectories. *Journal of Numerical Analysis, Industrial and Applied Mathematics*, 7(1-2):15–26, 2012.

[10] Uluc Saranli, Martin Buehler, and Daniel E Koditschek. Rhex: A simple and highly mobile hexapod robot. *The International Journal of Robotics Research*, 20(7):616–631, 2001.

[11] Alexander Spröwitz, Alexandre Tuleu, Massimo Vespignani, Mostafa Ajallooeian, Emilie Badri, and Auke Jan Ijspeert. Towards dynamic trot gait locomotion: Design, control, and experiments with Cheetah-cub, a compliant quadruped robot. *The International Journal of Robotics Research*, 32(8):932–950, 2013.